J Neurooncol (2009) 93:165–174
DOI 10.1007/s11060-008-9757-4

LABORATORY INVESTIGATION - HUMAN/ANIMAL TISSUE

# Incorporation of endothelial progenitor cells into the neovasculature of malignant glioma xenograft

**Hua-rong Zhang · Fei-lan Chen · Chen-ping Xu · Yi-fang Ping · Qing-liang Wang · Zi-qing Liang · Ji Ming Wang · Xiu-wu Bian**

Received: 6 April 2008 / Accepted: 17 November 2008 / Published online: 4 December 2008


**Abstract** Endothelial progenitor cells (EPCs) are important initiators of vasculogenesis in the process of tumor neovascularization. However, it is unclear how circulating EPCs contribute to the formation of tumor microvessels. In this study, we isolated $CD34^+/CD133^+$ cells from human umbilical cord blood (HUCB) and obtained EPCs with the capacities of forming colonies, uptaking acetylated low-density lipoprotein (ac-LDL), binding lectins and expressing vascular endothelial growth factor (VEGF) receptor 2 (VEGFR-2, KDR), CD31 and von Willebrand factor (vWF). These EPCs were actively proliferative and migratory, and could formed capillary-like tubules in response to VEGF. When injected into mice bearing subcutaneously implanted human malignant glioma, EPCs specifically accumulated at the sites of tumors and differentiated into mature endothelial cells (ECs), which accounted for 18% ECs of the tumor microvessels. The incorporation of circulating EPCs into tumor vessel walls significantly affected the morphology and structure of the vasculature. Our results suggest that circulating EPCs constitute important components of tumor microvessel network and contribute to tumor microvascular architecture phenotype heterogeneity.

**Keywords** Endothelial progenitor cells · Glioma · Angiogenesis · Vasculogenesis

Hua-rong Zhang, Fei-lan Chen and Chen-ping Xu—contributed equally to this study.

H.-r. Zhang · F.-l. Chen · C.-p. Xu · Y.-f. Ping · Q.-l. Wang · X.-w. Bian (✉)
Institute of Pathology and Southwest Cancer Center, Southwest Hospital, Third Military Medical University, Chongqing 400038, China
e-mail: bianxiuwu@263.net

Z.-q. Liang
Department of Obstetrics and Gynecology, Southwest Hospital, Third Military Medical University, Chongqing 400038, China

J. M. Wang
Laboratory of Molecular Immunoregulation, Cancer and Inflammation Program, Center for Cancer Research, National Cancer Institute at Frederick, Frederick, MD 21702, USA

## Introduction

The growth and progression of solid tumors are dependent on newly-formed microvessels, where niches for tumor cells as well as cancer stem cells exist [1–4]. Both angiogenesis and vasculogenesis contribute to tumor neovascularization, which provides oxygen and nutrients for tumor cell survival and proliferation [5–7]. Angiogenesis is a process of new capillary formation from pre-existing host blood vessels, while vasculogenesis is conducted by circulating endothelial progenitor cells (EPCs). However, it remains unclear whether and how vasculogenesis by EPCs incorporates into angiogenesis by sprouting pre-existing endothelial cells (ECs) in the process of neovascularization.

Tumor microvessls are structurally diverse, which forms the basis for tumor microvascular architecture phenotype heterogeneity (T-MAPH) [8] and differential potential targets for anti-cancer therapy. Unfortunately, the existing antiangiogenic agents have not shown consistently effective tumor suppression in clinical trials [9–11]. This raises the possibility that the complexity of T-MAPH needs to be taken into consideration because T-MAPH may consist of ECs derived from different sources such as from existing host vessels and circulating precursors in the blood.

In this study, we examined the possible incorporation of EPCs in host circulation into glioma neovascularization.

We found EPCs from human umbilical cord blood (HUCB) were present in newly-formed microvessels in gliomas subcutaneously implanted into SCID mice, in addition to their capacity of forming capillary-like tubules in Matrigel in vitro. Moreover, both ECs differentiated from implanted human EPCs and host ECs participating in neovascularization contributed to the formation of T-MAPH.

## Materials and methods

### Isolation and culture of EPCs

HUCB was obtained from the informed and consenting donors at Southwest Hospital, Third Military Medical University, Chongqing, China. The umbilical cords were clamped and cord blood collection was performed *ex utero* according to standard hospital procedures.

EPCs were isolated and cultured according to previous description [12, 13]. Briefly, 70–80 ml HUCB from each donor was collected into a sterile bag containing 28 ml citrate phosphate dextrose solution. Mononuclear cells (MNCs) were isolated by density gradient centrifugation with Histopaque-1077 (Sigma, St. Louis, MO), seeded in culture flasks or on glass cover slips pre-coated with 10 μg/ml human fibronectin (Sigma) and maintained in EGM-2 BulletKit system (Clonetics, San Diego, CA) consisting of endothelial basal medium (EBM-2), 5% fetal bovine serum, human epidermal growth factor (hEGF), vascular endothelial growth factor (VEGF), human basic fibroblast growth factor (hbFGF), insulin-like growth factor-1 (IGF-1), hydrocortisone, GA-1000 (gentamicin sulfate and amphotericin), ascorbic acid and heparin. On day 2, non-adherent cells were removed, followed by addition of new medium. Thereafter, media were changed every 3 days. When adherent cells formed colonies and continued to grow into cobblestone-like monolayer, the cells were reseeded in 6-well plates pre-coated with 10 μg/ml human fibronectin at a density of 400 cells/well to acquire secondary colonies.

### Characterization of EPCs

#### *Flow cytometry*

Freshly-isolated MNCs and those collected after 4 days of culture were incubated with fluorescein isothiocyanate (FITC)-conjugated mouse monoclonal anti-human CD34 antibody (Miltenyi Biotech, Bergisch Gladbach, Germany) and phycoerythrin (PE)-conjugated mouse monoclonal anti-human CD133/1 antibody (Miltenyi Biotech) for 10 min at 4°C. FITC-conjugated anti-mouse IgG2a (Miltenyi Biotech) and PE-conjugated anti-mouse IgG1 antibody (R&D Systems, Wiesbaden, Germany) were used as isotype controls. The cells were then washed with PBS containing 0.5% bovine serum albumin (BSA) and 2 mM ethylenediamine tetraacetic acid (EDTA). Quantitative analyses were performed using a FACS SCAN flow cytometer and CellQuest software (Becton Dickinson, Heidelberg, Germany). The EPCs were calculated as percentage of all MNCs. Each analysis included 100,000 events.

#### *Immunofluorescent staining for CD34, CD133 and KDR*

To determine the expression of CD34, CD133 and KDR, EPCs reseeded on coverslips for 8 or 15 days were fixed in 2% paraformaldehyde for 15 min. For direct immunofluorescent staining, the cells were incubated with FcR Blocking Reagent (Miltenyi Biotech) and then in a specific antibody-cocktail diluted in PBS containing 0.5% BSA as well as 2 mM EDTA at 37°C for 30 min. The specific antibody-cocktail consisted of either (1) FITC-conjugated mouse monoclonal anti-human CD34 (1:11), and PE-conjugated mouse monoclonal anti-human CD133/1 (1:11), or (2) FITC-conjugated mouse monoclonal anti-human CD34 (1:11), and allophycocyanin (APC)-conjugated mouse monoclonal anti-human KDR (1:3.5) (R&D Systems) antibodies. FITC-conjugated mouse IgG2a and PE-conjugated mouse IgG1 or APC-conjugated mouse IgG1 were used as isotype controls. Samples were mounted with 50% glycerol in carbonate buffer and examined by laser confocal scanning microscopy.

#### *Assays for ac-LDL uptake and lectin binding*

To evaluate the ability of acetylated low-density lipoprotein (ac-LDL) uptake and binding of lectin on EPCs, cells cultured for 11 days were washed with EBM-2 (serum-free medium) and incubated with 1,1′-dioctadecyl 3,3,3′,3′-tetramethylindocarbocyanine perchlorate (DiI)-ac-LDL (Molecular Probes, Leiden, Netherlands) at a concentration of 10 μg/ml in EBM-2 for 3 h at 37°C. Then, the cells were fixed with 2% paraformaldehyde for 10 min and incubated with FITC-conjugated lectin from Ulex europeus (UEA-1) (Sigma, Deisenhofen, Germany) at a concentration of 10 μg/ml in EBM-2 for additional 1 h at 37°C. After washing, double-positive (Dil-ac-LDL and FITC-UEA-1) cells were observed under laser confocal scanning microscopy.

#### *Immunocytochemistry for CD31 and vWF*

For detection of differentiation potential of EPCs, cells after 40 days of culture were incubated with normal goat serum for 30 min at 37°C in a humidified chamber, and then were incubated overnight with monoclonal mouse

anti-human CD31 antibody (1:50 dilution; BD Pharmingen) or an anti-human von Willebrand factor (vWF) (1:100 dilution; Zhongshan Jingqiao Tech, Beijing, China) at 4°C. FITC-conjugated goat anti-mouse IgG (1:100 dilution; Zhongshan Jingqiao Tech) was used to detect CD31 and biotinylated goat anti-rabbit IgG, peroxidase-labeled ultrastreptavidin as well as DAB (Zhongshan Jingqiao Tech) were used to detect vWF. The stained cells were observed under laser confocal scanning microscopy as well as light microscopy.

*Assays for EPC vasculogenesis*

EPCs cultured in EGM-2 BulletKit system for 10 days were transferred to EBM-2 for 24 h and harvested using 1 mmol/l EDTA for assays of proliferation, migration, tubulogenesis and in vivo formation of vasculature.

*Proliferation assay*

EPC proliferation was determined by 3-(4,5-dimethylthiazol-2-yl)-2,5-diphenyltetrazolium bromide (MTT) assays. 1,000 EPCs in 200 μl/well were cultured in EBM-2 with or without 50 ng/ml VEGF (Peprotech, UK) in 96-well culture plates pre-coated with 10 μg/ml human fibronectin. After being cultured for 24, 48, or 72 h, EPCs were supplemented with 20 μl MTT (5 mg/ml, Sigma) and incubated for another 4 h. The supernatant was discarded and the EPC preparations were shacked in 200 μl dimethyl sulfoxide (DMSO, Sigma) for 10 min, followed by measurement of optical density value at 490 nm. Results from three independent experiments in triplicates were presented.

*Migration assay*

EPC migration was evaluated using a modified Boyden chemotaxis chamber assay. Polyvinylpyrrolidone-free polycarbonate filter transwell inserts (8 μm pores; Costar, Cambridge, MA) were incubated with 10 μg/ml human fibronectin and air dried. Inserts were placed in a 24-well plate containing 500 μl/well EBM-2 medium with or without 50 ng/ml VEGF. EPCs (10,000 cells/well) in EBM-2 were added to the upper chamber of the inserts. After 24 h at 37°C, non-migratory cells were removed from the upper chamber by wiping the upper surface of the filter and the migrated cells on the lower side of the filter were washed with PBS and fixed for 10 min with 2% paraformaldehyde. For quantification, the migrated cells were stained with Diff-Quik (American Scientific Products, Edison, NJ, USA) and the number of migrated cells was counted in five random high power (200×) fields per insert.

*Tubulogenesis in Matrigel*

To examine the ability of EPCs to participate in the formation of vascular network in vitro, growth factor reduced Matrigel (Becton Dickinson Labware) was placed in a 24-well plate at 37°C for 1 h for solidification, EPCs were then replated (30,000 cells/well) on top of the solidified Matrigel. Cells were grown with EBM-2 containing 50 ng/ml of VEGF or EBM-2 alone, and incubated at 37°C for 24 h. The tubule structure formed by EPCs was photographed at 200× magnification under phase-contrast microscopy.

*Incorporation of EPCs into tumor vasculature*

We utilized a glioblastoma transplantation model to study the ability of EPCs forming endothelial capillaries in vivo. Briefly, human U87 glioma xenografts were grown subcutaneously after injection of $6 \times 10^6$ cells (ATCC, Manassas, VA, USA) into the flanks of sublethally irradiated (350 cGy) 6-week-old SCID mice (Laboratory Animal Center, Third Military Medical University). After the appearance of tumors (day 7 after implantation), EPCs ($5 \times 10^5$/100 μl) were injected into tumor-bearing mice via tail vein ($n = 6$). Tumor-bearing mice without EPCs were used as control group ($n = 5$). The animals were raised under specific pathogen-free (SPF) condition. The tumor volumes were measured by a vernier caliper and calculated by the formula: Volume $= l$ (length) $\times w^2$ (width)/2. Twenty-eight days later, the animals were euthanized and tumors were removed and frozen in liquid nitrogen for inclusion into OCT (optimal cutting temperature) compound. Cryosections of 10 μm were prepared. In order to quantitate EPCs incorporation, tumor cryosections were double labeled with a monoclonal mouse anti-human CD31 antibody (1:50 dilution; BD Pharmingen, San Diego, CA) and a monoclonal rat anti-mouse CD31 antibody (1:50 dilution; BD Pharmingen). Cryosections were subsequently washed and labeled simultaneously with tetraethyl rhodamine isothiocyanate (TRITC)-conjugated goat anti-mouse IgG and FITC-conjugated goat anti-rat IgG (1:100 dilution; Zhongshan JingqiaoTech, Beijing, China). Finally, cellular nuclei were counterstained by 4′,6-diamidino-2-phenylindole (DAPI, Sigma). The sections were examined under laser confocal scanning microscopy. At low power field (40×), six most intensely vascularized fields (so called "hot spots") were randomly selected under laser confocal scanning microscopy. Microvessel counting of these areas was performed at high power field (100×) by Image Proplus 6.0 software and the mean of microvessel number expressing human CD31 in the six fields was obtained. Then, the mean of total number of microvessels expressing both human CD31 and mouse CD31 in the same areas was

calculated. Finally, the proportion of anti-human CD31 in total vessels was calculated. The relative contribution of engrafted EPCs to tumor vasculature was estimated by dividing total number of anti-human CD31-positive vessels by combined number of anti-human and mouse CD31-positive vessels.

In order to confirm the incorporation of transplanted EPCs into growing tumor vasculature, EPCs ($5 \times 10^5$) were labeled in vitro with cell tracker carboxyfluorescein diacetate succinimidyl ester (CFSE, Molecular Probes) according to the manufacturer's instructions and suspended in 100 μl PBS, then injected via tail vein into sublethally irradiated (350 cGy) 6-week-old SCID mice ($n = 5$). U87 cells ($6 \times 10^6$) were injected on the same day in the right flanks of the mice. When tumors were palpable, the tumors, spleens and livers were harvested and cryosections of 10–60 μm were prepared. The cryosections were examined under laser confocal scanning microscopy to visualize the distribution and localization of engrafted CFSE-labeled EPCs. To test if the engrafted EPCs possessed EC phenotype and contributed to microvascular heterogeneity in morphology and 3D spatial distribution, tumor cryosections containing green fluorescent EPCs were also immunostained with a monoclonal mouse anti-human CD31 antibody or a monoclonal rat anti-mouse CD31 antibody overnight at 4°C, followed by rinsing with PBS and incubating for 1 h with TRITC-conjugated goat anti-mouse IgG, Cy5-conjugated goat anti-mouse IgG or TRITC-conjugated goat anti-rat IgG (1:100 dilution; Zhongshan Jingqiao Tech). After washing with PBS and counterstained with DAPI for revealing nuclei, the sections were examined with laser confocal scanning microscopy. Cryosections of 60 μm were scanned at 0.5 μm intervals to reconstruct three-dimension of the tumor vessels by an image analysis software (3D projection).

Additionally, fresh tumor tissues were minced and digested with protease (0.05% w/v) (Roche, Mannheim, Germany) at 37°C for 1 h with gentle shaking, washed twice with PBS, and digested again with collagenase/diapase (0.035% w/v) (Roche) at 37°C for 1 h. Cells were filtered through 75 μm sterile steel mesh, spun down at 1,500 rpm, and resuspended in PBS. These cells were labeled with anti-human CD31 or anti-mouse CD31 antibody and assessed by FACS.

We utilized an orthotopic model to determine if EPCs contributed to tumor growth in the microenvironment of brain glioma. Intracranial gliomas were obtained by injecting $1 \times 10^5$ U87 cells in the brain of SCID mice ($n = 5$) according to previous description [14]. Tumors were harvested when animals showed signs of neurological impairment. The animal experiments were approved by the Ethics Committee of our institution.

### Statistical analysis

All data are presented as mean ± s.d. Differences between group means were assessed by an unpaired Student's *t*-test for single comparisons or by ANOVA for multiple comparisons using SPSS 13.0. *P*-values less than 0.05 were considered as statistically significant.

## Results

### EPCs formed colonies and functionally differentiate to ECs

During 3–7 days of culture, MNCs attached to the flask bottom became elongated and showed linear cord-like structures (Fig. 1A). On day 9 through 17, the cells formed colonies (Fig. 1B). The colony-forming cells were reseeded, and their offspring cells produced secondary colonies (Fig. 1C). Cells from the secondary colones gradually evolved into cobblestone-like monolayer reaching confluence (Fig. 1D).

In order to define the nature of potential EPCs, flow cytometry was performed with isolated MNCs cultured on day 0 through day 4. In freshly isolated MNCs, 1.20% expressed CD133, 1.85% CD34, and 1.06% were CD34/CD133 positive (Fig. 2A). After culture for 4 days, the expression of CD133 decreased to 0.78% which implied MNCs began to differentiate, while CD34 increased to 3.85%, and CD34/CD133 decreased to 0.26% (Fig. 2B). Coexpression of CD34/CD133 or CD34/KDR on EPCs was examined on day 8 and 15. During this period, EPCs continued to positively express CD34 and KDR, while CD133 became less positive (Fig. 3A). Most adherent cells (>95%) after 11 days in culture showed uptake of DiI-ac-LDL and binding of FITC-UEA-1 (Fig. 3B). After 40 days of culture, EPCs were found to express markers of mature ECs, CD31 and vWF (Fig. 3C, D).

### VEGF promoted EPC proliferation, migration and tubulogenesis

When stimulated with VEGF (50 ng/ml), EPCs showed increased cell number as compared to control group at 24, 48, and 72 h ($P < 0.05$) (Fig. 4). In addition, when stimulated with VEGF (50 ng/ml) for 24 h, the number of migrated EPCs significantly increased ($P < 0.05$) (Fig. 5A, B). Furthermore, in Matrigel tubule assays, VEGF stimulated EPCs formed increased number of tubules as compared with cells in the absence of VEGF ($P < 0.05$) (Fig. 6A, B).

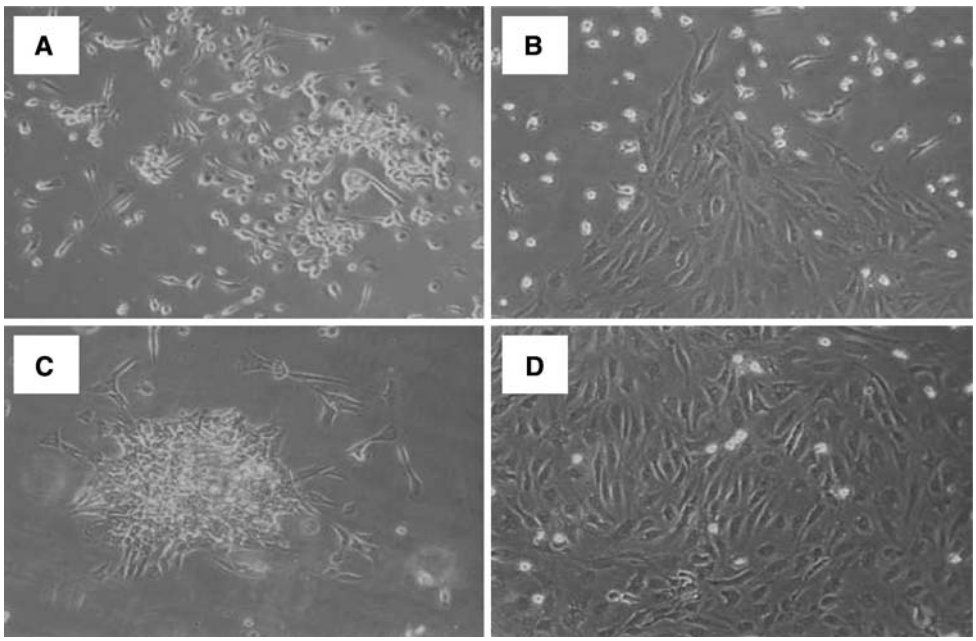


**Fig. 1** Morphology of EPCs in culture. **A** Adherent and elongated cells on the culture days 3–7. **B** Increased EPC colonies with sprouting cells on the days 9–17. **C** Secondary colonies formed by reseeded EPCs. **D** Cobblestone-like monolayer. Phase-contrast light microscopy, 200×

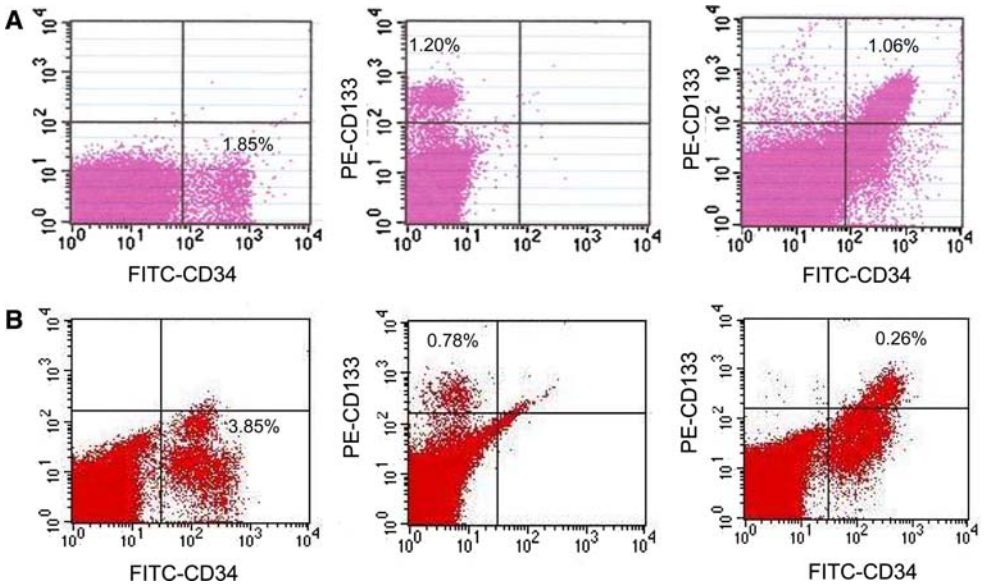


**Fig. 2** Phenotype of EPCs detected by flow cytometry. **A** The expression of CD133, CD34, and CD133/CD34 by freshly-isolated MNCs. **B** The expression of CD133, CD34, and CD133/CD34 by MNCs after 4-day culture

## EPCs incorporated into newly-formed microvessels in vivo

In order to evaluate the capacity of cultured EPCs to participating in neovascularization in transplanted tumors, we utilized a subcutaneous glioblastoma xenograft model. To exclude possible competition by autologous EPCs with engrafted EPCs for incorporation into tumor vasculature [15], SCID mice used in the study were sublethally irradiated (350 cGy) before implantation with U87 glioma cells. Subcutaneous tumors were formed 7 days after transplantation, and then human EPCs were injected via tail vein. All the SCID mice that received sublethal irradiation survived during period of experiment. On day 21 after U87 implantation, the average volume of subcutaneous tumors in SCID mice with EPCs was 244 $mm^3 \pm 38$ $mm^3$, significantly larger than that in SCID mice without EPCs (122 $mm^3 \pm 20$ $mm^3$). Similarly, the average volume (24.21 $mm^3 \pm 4.64$ $mm^3$) of intracranial tumors with EPCs was significantly larger than that of intracranial tumors without EPCs (16.24 $mm^3 \pm 3.98$ $mm^3$). This result suggested that EPCs might promote more tumor growth. We harvested subcutaneous tumors on day 28. Immunofluorescence revealed numerous vessels in subcutaneous tumors in which human CD31-expressing cells were found in linear or tubular arrangement in tumor tissues (Fig. 7A).

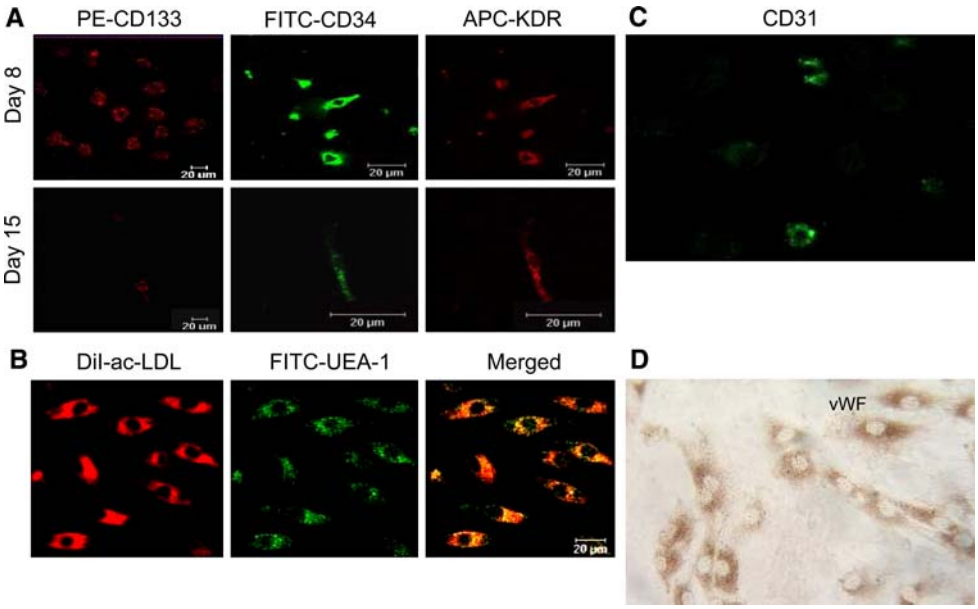


**Fig. 3** The expression of endothelial markers by EPCs. **A** The expression of CD34 and KDR on the days 8–15. **B** Uptaking of DiI-ac-LDL and binding FITC-UEA-1 by MNCs cultured for 11 days. **C**, **D** The expression of CD31 (**C**) and vWF (**D**) by EPCs on the day 40. **A–C** Immunofluorescence under laser confocal scanning microscopy. **D** Immunoperoxydase labeling, under light microscopy (200×)

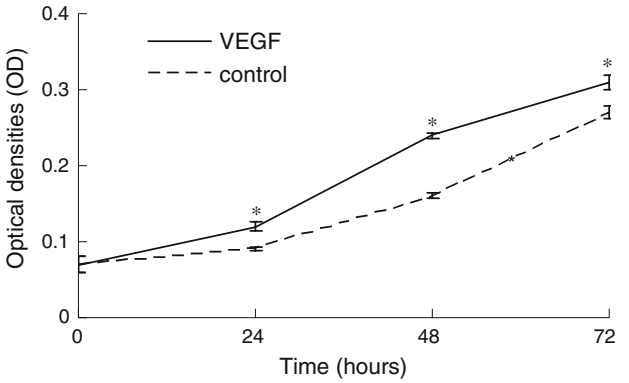


**Fig. 4** Growth of EPCs with and without VEGF. * Significant increase of VEGF-stimulated EPCs proliferation as compared to those without VEGF stimulation ($P < 0.05$)

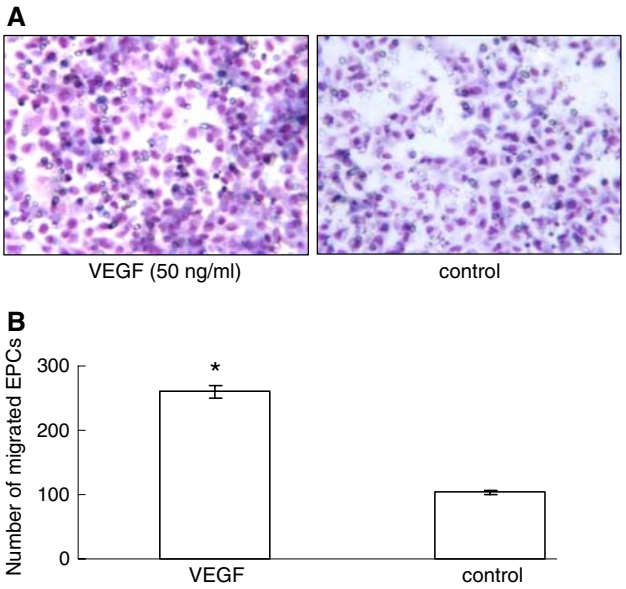


**Fig. 5** The effect of VEGF on EPCs migration. **A**, **B** Significantly increased migration of EPCs in response to 50 ng/ml VEGF. * $P < 0.05$ as compared to cell migration in the absence of VEGF

Therefore, injected human EPCs were integrated into the endothelial lining of the tumor microvasculature. For quantification, we calculated the percentage of vessels of human origin in tumor-associated vessels. Vessels expressing human CD31 accounted for 18.68% ± 1.32% of the total vessels, suggesting significant contribution of EPCs to tumor neovascularization. The incorporation of EPCs was also demonstrated by the presence of CFSE-labeled EPCs along human CD31-expressing vascular channels in subcutaneous tumors (Fig. 7B). To evaluate the distribution of transplanted EPCs in non-tumoral organs in tumor-bearing mice, we examined CFSE-labeled cells in cryosections of the spleen and liver. No CFSE-labeled EPCs were detected in the spleen and liver suggesting marked tropism of EPCs for tumors. FACS revealed that ECs from the host blood vessels represented 0.55% among cells from implanted tumor tissues and tumor ECs from implanted human EPCs represented 0.07%. Thus ECs derived from donor EPCs represented a distinct population (11.3% of all ECs in tumor vessels). We examined the role of engrafted EPCs in microvascular architecture by immunofluorescence and three-dimensional reconstruction technology. We found that the vasculature partly incorporated by implanted EPCs were aberrant in morphology showing strip-like structure, arborization, or serpentine sinusoid structure. ECs derived from human EPCs mostly localized at the branching points of the microvessels emanating from mother vessels (Fig. 8A). Three-dimensional chimeric vascular network

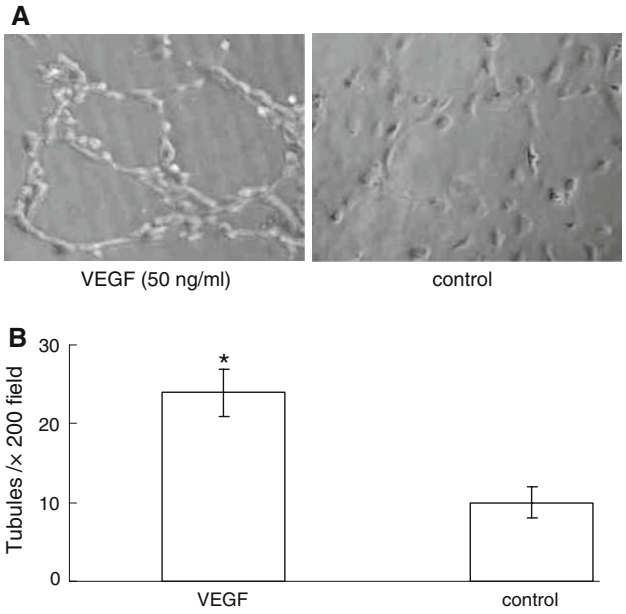


**Fig. 6** The effect of VEGF on tubulogenesis of EPCs in Matrigel. Increased number of tubules formed by EPCs with stimulation by VEGF (**A**), * $P < 0.05$ as compared to cells in the absence of VEGF (**B**)

containing $CFSE^+$ ECs was chaos with different branches, lengths and angles, $CFSE^+$ ECs linked mouse ECs in branches to form thickened vessels of multicellular clusters and or a blind loop (Fig. 8B). These results suggested the contribution of ECs to the microvascular architecture heterogeneity.

## Discussion

The study by Asahara et al. [16] demonstrated for the first time that purified $CD34^+$ progenitor cells from adult peripheral blood could differentiate ex vivo to exhibit an endothelial phenotype. These cells were thereafter called EPCs. Besides from peripheral blood, EPCs have also been collected from adult bone marrow, HUCB, and human fetal liver [17–19]. More recently, HUCB became a common source of EPCs. Accumulating evidence indicates that EPCs are actively recruited to sites of tumor, trauma, inflammation and ischemia, where the cells differentiate in situ into mature ECs and integrate into new blood vessels [20–22].

EPCs are immunologically identified by cell surface markers and functionally by tubulogenesis. Peichev et al. [17] identified a subset of endothelial precursors from circulating $CD34^+$ cells, which express VEGFR-2 and AC133 (CD133). More recent studies define primitive EPCs derived from bone marrow as $CD133^+/CD34^+/KDR^+$. $CD133^+$ EPCs incubated with medium containing angiogenic growth factors progressively lost CD133 expression with increased cell surface mature EC makers such as vWF, CD31, CD105 and vascular endothelial (VE)

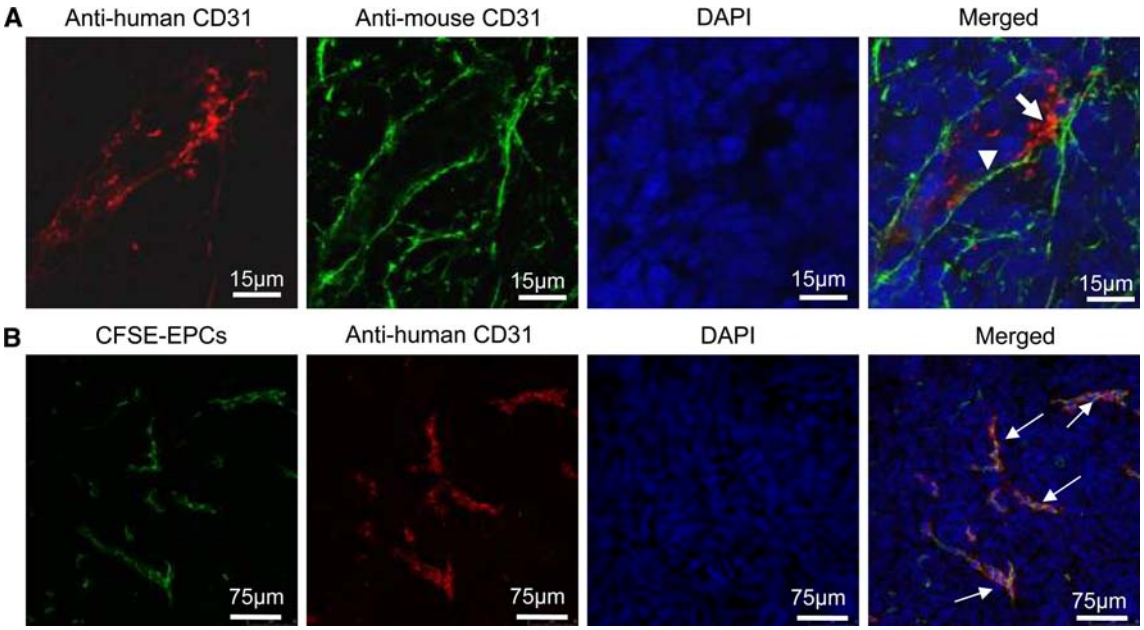


**Fig. 7** EPC incorporation into newly-formed microvessels in tumor xenografts. Human EPCs were injected via tail vein into SCID mice bearing subcutaneously implanted gliomas. Tumors were sectioned on day 28. **A** Double staining with anti-human CD31 and anti-mouse CD31 antibodies revealing ECs derived from human EPCs (human CD31) that formed new microvessels (*arrow*) or lined the lumen of murine vessels (*arrowhead*). **B** ECs differentiated from CFSE-labeled EPCs in microvessel walls positive for human CD31 in tumor. ECs were revealed in yellow color (*arrows*)

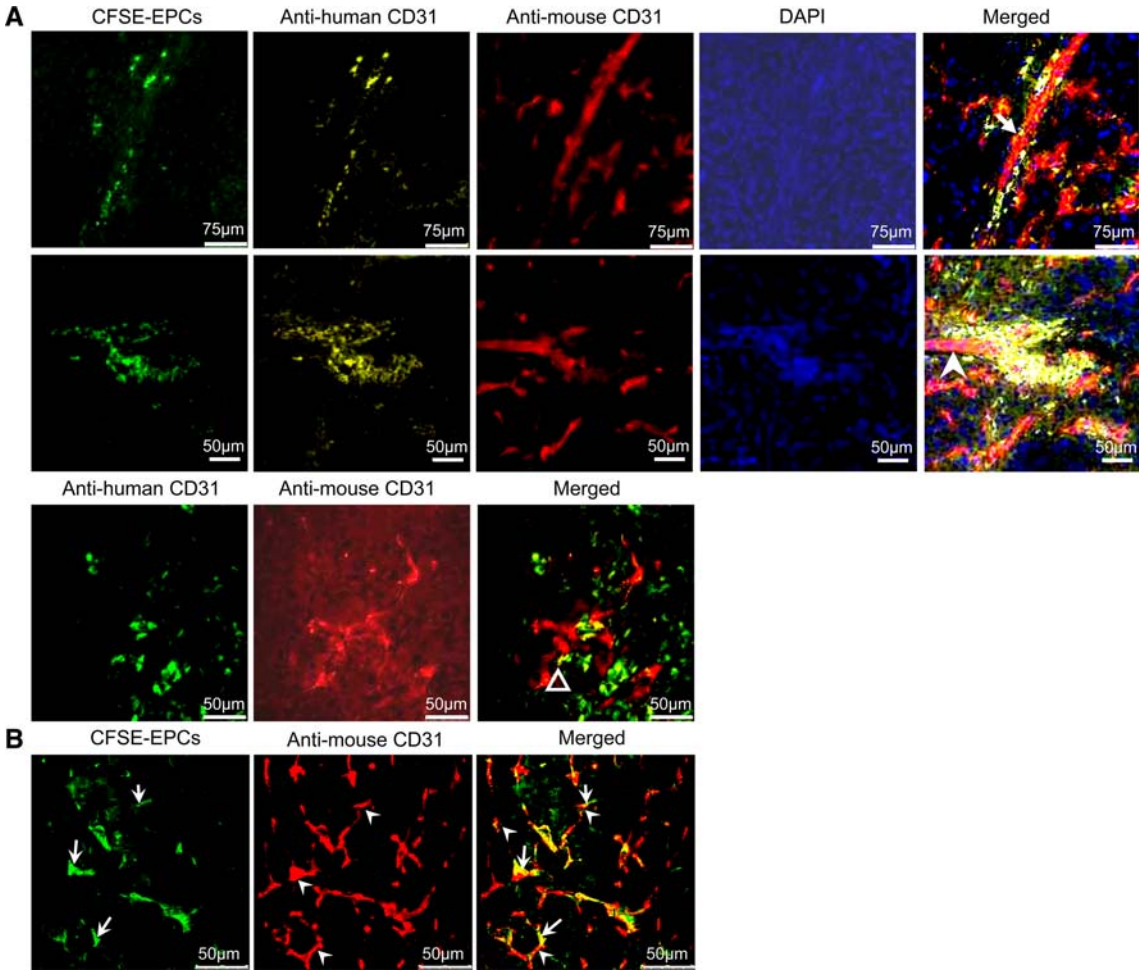


**Fig. 8** Contribution of EPC to T-MAPH. **A** Double staining with anti-human CD31 and anti-mouse CD31 antibodies revealing $CFSE^+$ cells expressed human CD31 that form strip structure (*arrow*), branching pattern (*arrowhead*), and sinusoid structure (*triangle*). **B** Three-dimensional reconstruction of the vessels revealing chaos chimeric vascular network contained of $CFSE^+$ ECs (*arrow*) and mouse-derived ECs (*arrowhead*) with different branches, lengths and angles

cadherin (VE-cadherin) [18]. In addition, Yoder et al. [23] redefined EPCs by their capacity to form colonies with robust proliferation potential in vitro and perfused vessel formation in vivo. Therefore, EPCs are believed to possess the characteristic as being non-EC that can give rise to ECs with clonal expansion and stem cell properties [24].

We have shown that potential EPCs isolated from HUCB incorporated into tumor neovasculature after systemic injection. EPCs expressed progenitor cell markers CD34 and CD133 and possessed the capacity of generating colonies in short term culture. These EPCs exhibited cobblestone-like morphology with phenotypic and functional features similar to mature ECs. These results suggest that EPCs thus obtained may serve as valuable tools for studies of mechanisms of neovascularization in vivo.

It has been reported that bone marrow-derived circulating EPCs contribute to neovascularization in adult. This is in contrast to the hypothesis that vasculogenesis occurs only during the embryonic period [25]. EPCs can be mobilized from bone marrow into the blood stream by a variety of angiogenic growth factors such as VEGF and chemokines such as stromal derived factor 1 (SDF-1). They subsequently are recruited and incorporated into vessel walls at the sites of active physiological or pathological vasculogenesis such as endometrial neovascularization, tissue ischemia, vascular trauma as well as cancer [21, 26, 27]. EPCs have been detected at increased frequency in the peripheral blood circulation of cancer patients [28, 29] and the levels of EPCs may serve as indicators of tumor progression and patient prognosis. EPCs may also indirectly promote vasculogenesis by releasing growth factors, such as VEGF, hepatocyte growth factor (HGF), and granulocyte (macrophage) colony stimulating factor (GM-CSF) [30], etc.

Anti-angiogenic therapies have become one of the most promising approaches in the anti-cancer drug development. Antiangiogenic drugs exert their effects on cancer progression through several mechanisms: (a) by interfering

with the activity of angiogenic factors, their receptors or downstream signaling pathways; (b) by upregulating or delivering endogenous inhibitors, and (c) by directly targeting tumor vasculature [31, 32]. Although experimental models offered promising therapeutic results, many anti-angiogenesis agents fail to show consistent tumor suppressing results in cancer patients. These discrepancies in results obtained in preclinical versus clinical studies call for better understanding of the mechanisms of tumor neovascularization.

Tumor vessels are structurally and functionally abnormal, with tumor blood flow in chaotic and variable conditions [33]. Tumor vasculature is highly disorganized, tortuous and dilated, with uneven diameter, excessive branching and shunts. Such abnormality may cause difficulties in achieving effective anti-angiogenesis cancer therapy [34]. We proposed the concept of tumor microvascular architecture phenotype heterogeneity (T-MAPH) based on the observations that tumor blood vessels are diverse and heterogeneous in organization, morphology, density and 3D spatial distribution [8]. Our present study indicates that the chimeric vasculature incorporated by implanted EPCs showed aberrantly morphologic diversity such as arborization, strip-like structure, and serpentine sinusoid structure and chaos three-spatial distribution with different branches, lengths and angles. These results indicate the contribution of EPCs to tumor neovascularization that may be involved in the formation of T-MAPH.

Malignant gliomas are characterized by the presence of abundant newly-formed microvessels. In previous studies, we have shown that tumor cells especially those surrounding microvessels in very aggressive glioblastomas, are highly positive for VEGF staining thus may actively recruit ECs, support their proliferation, and promote the formation of new vasculature. The exposure of ECs to excessive VEGF may also result in the formation of T-MAPH [8]. Circulating EPCs show similar responses to VEGF within tumor tissues. In the present study, EPCs responded to VEGF by proliferation, migration and tubule formation in vitro. HUCB-derived EPCs when injected systemically incorporated into neovessels of tumors formed by VEGF-producing glioblastoma cells. These findings provide a basis for better understanding the mechanism of T-MAPH formation and the potential for the development of more effective anti-cancer vasculature agents.

**Acknowledgements** We thank Mrs Wei Sun and Miss Li-Ting Wang (Central Laboratory, Third Military Medical University, Chongqing, China) for their technical assistance in laser confocal scanning microscopy. This study was supported by grants from the National Basic Research Program of China (973 Program, No. 2006CB708503) and the Outstanding Scholar Fellowship of P.L.A. (No.06J012).

## References

1. Fischer I, Gagner JP, Law M, Newcomb EW, Zagzag D (2005) Angiogenesis in gliomas: biology and molecular pathophysiology. Brain Pathol 15:297–310. doi:10.1111/j.1750-3639.2005.tb00115.x
2. Cogle CR, Scott EW (2004) The hemangioblast: cradle to clinic. Exp Hematol 32:885–890. doi:10.1016/j.exphem.2004.07.014
3. Nikolova G, Strilic B, Lammert E (2007) The vascular niche and its basement membrane. Trends Cell Biol 17:19–25. doi:10.1016/j.tcb.2006.11.005
4. Calabrese C, Poppleton H, Kocak M, Hogg TL, Fuller C, Hamner B et al (2007) A perivascular niche for brain tumor stem cells. Cancer Cell 11:69–82. doi:10.1016/j.ccr.2006.11.020
5. Aghi M, Chiocca EA (2005) Contribution of bone marrow-derived cells to blood vessels in ischemic tissues and tumors. Mol Ther 12:994–1005. doi:10.1016/j.ymthe.2005.07.693
6. Davidoff AM, Ng CY, Brown P, Leary MA, Spurbeck WW, Zhou J et al (2001) Bone marrow-derived cells contribute to tumor neovasculature and, when modified to express an angiogenesis inhibitor, can restrict tumor growth in mice. Clin Cancer Res 7:2870–2879
7. Ruzinova MB, Schoer RA, Gerald W, Egan JE, Pandolfi PP, Rafii S et al (2003) Effect of angiogenesis inhibition by Id loss and the contribution of bone-marrow-derived endothelial cells in spontaneous murine tumors. Cancer Cell 4:277–289. doi:10.1016/S1535-6108(03)00240-X
8. Bian XW, Chen JH, Jiang XF, Wang QL, Zhang X (2004) Angiogenesis as an immunopharmacologic target in inflammation and cancer. Int Immunopharmacol 4:1537–1547. doi:10.1016/j.intimp.2004.07.017
9. Shaked Y, Bertolini F, Man S, Rogers MS, Cervi D, Foutz T et al (2005) Genetic heterogeneity of the vasculogenic phenotype parallels angiogenesis: implications for cellular surrogate marker analysis of antiangiogenesis. Cancer Cell 7:101–111. doi:10.1016/j.ccr.2004.11.023
10. Quesada AR, Munoz-Chapuli R, Medina MA (2006) Anti-angiogenic drugs: from bench to clinical trials. Med Res Rev 26:483–530. doi:10.1002/med.20059
11. Eichhorn ME, Strieth S, Dellian M (2004) Anti-vascular tumor therapy: recent advances, pitfalls and clinical perspectives. Drug Resist Updat 7:125–138. doi:10.1016/j.drup.2004.03.001
12. Murohara T, Ikeda H, Duan J, Shintani S, Sasaki K, Eguchi H et al (2000) Transplanted cord blood-derived endothelial precursor cells augment postnatal neovascularization. J Clin Invest 105:1527–1536. doi:10.1172/JCI8296
13. Kalka C, Masuda H, Takahashi T, Kalka-Moll WM, Silver M, Kearney M et al (2000) Transplantation of ex vivo expanded endothelial progenitor cells for therapeutic neovascularization. Proc Natl Acad Sci USA 97:3422–3427. doi:10.1073/pnas.070046397
14. Ping YF, Yao XH, Chen JH, Liu H, Chen DL, Zhou XD et al (2007) The anti-cancer compound Nordy inhibits CXCR4-mediated production of CXCL8 and VEGF by malignant human glioma cells. J Neurooncol 84:21–29. doi:10.1007/s11060-007-9349-8
15. Ferrari N, Glod J, Lee J, Kobiler D, Fine HA (2003) Bone marrow-derived, endothelial progenitor-like cells as angiogenesis-selective gene-targeting vectors. Gene Ther 10:647–656. doi:10.1038/sj.gt.3301883
16. Asahara T, Murohara T, Sullivan A, Silver M, van der Zee R, Li T et al (1997) Isolation of putative progenitor endothelial cells for angiogenesis. Science 275:964–967. doi:10.1126/science.275.5302.964
17. Peichev M, Naiyer AJ, Pereira D, Zhu Z, Lane WJ, Williams M et al (2000) Expression of VEGFR-2 and AC133 by circulating

human CD34$^+$ cells identifies a population of functional endothelial precursors. Blood 95:952–958
18. Quirici N, Soligo D, Caneva L, Servida F, Bossolasco P, Deliliers GL (2001) Differentiation and expansion of endothelial cells from human bone marrow CD133(+) cells. Br J Haematol 115:186–194. doi:10.1046/j.1365-2141.2001.03077.x
19. Shi Q, Rafii S, Wu MH, Wijelath ES, Yu C, Ishida A et al (1998) Evidence for circulating bone marrow-derived endothelial cells. Blood 929:362–367
20. Machein MR, Renninger S, de Lima-Hahn E, Plate KH (2003) Minor contribution of bone marrow-derived endothelial progenitors to the vascularization of murine gliomas. Brain Pathol 13:582–597. doi:10.1111/j.1750-3639.2003.tb00487.x
21. Asahara T, Masuda H, Takahashi T, Kalka C, Pastore C, Silver M et al (1999) Bone marrow origin of endothelial progenitor cells responsible for postnatal vasculogenesis in physiological and pathological neovascularization. Circ Res 85:221–228
22. Asai J, Takenaka H, Kusano KF, Ii M, Luedemann C, Curry C et al (2006) Topical sonic hedgehog gene therapy accelerates wound healing in diabetes by enhancing endothelial progenitor cell-mediated microvascular remodeling. Circulation 113:2413–2424. doi:10.1161/CIRCULATIONAHA.105.603167
23. Yoder MC, Mead LE, Prater D, Krier TR, Mroueh KN, Li F et al (2007) Re-defining endothelial progenitor cells via clonal analysis and hematopoietic stem/progenitor cell principals. Blood 109:1801–1809. doi:10.1182/blood-2006-08-043471
24. Urbich C, Dimmeler S (2004) Endothelial progenitor cells functional characterization. Trends Cardiovasc Med 14:318–322. doi:10.1016/j.tcm.2004.10.001
25. Isner JM, Asahara T (1999) Angiogenesis and vasculogenesis as therapeutic strategies for postnatal neovascularization. J Clin Invest 103:1231–1236. doi:10.1172/JCI6889
26. Santarelli JG, Udani V, Yung CY, Cheshier S, Wagers A, Brekken RA et al (2006) Incorporation of bone marrow-derived flk-1-expressing CD34$^+$ cells in the endothelium of tumor vessels in the mouse brain. Neurosurgery 59:374–382. doi:10.1227/01.NEU.0000222658.66878.CC
27. Yamaguchi J, Kusano KF, Masuo O, Kawamoto A, Silver M, Murasawa S et al (2003) Stromal cell-derived factor-1 effects on ex vivo expanded endothelial progenitor cell recruitment for ischemic neovascularization. Circulation 107:1322–1328. doi:10.1161/01.CIR.0000055313.77510.22
28. Mancuso P, Burlini A, Pruneri G, Goldhirsch A, Martinelli G, Bertolini F (2001) Resting and activated endothelial cells are increased in the peripheral blood of cancer patients. Blood 97:3658–3661. doi:10.1182/blood.V97.11.3658
29. Beerepoot LV, Mehra N, Vermaat JS, Zonnenberg BA, Gebbink MF, Voest EE (2004) Increased levels of viable circulating endothelial cells are an indicator of progressive disease in cancer patients. Ann Oncol 15:139–145. doi:10.1093/annonc/mdh017
30. Rehman J, Li J, Orschell CM, March KL (2003) Peripheral blood "endothelial progenitor cells" are derived from monocyte/macrophages and secrete angiogenic growth factors. Circulation 107:164–1169. doi:10.1161/01.CIR.0000058702.69484.A0
31. McCarty MF, Liu W, Fan F, Parikh A, Reimuth N, Stoeltzing O et al (2003) Promises and pitfalls of anti-angiogenic therapy in clinical trials. Trends Mol Med 9:53–58. doi:10.1016/S1471-4914(03)00002-9
32. Rafii S, Lyden D, Benezra R, Hattori K, Heissig B (2002) Vascular and haematopoietic stem cells: novel targets for anti-angiogenesis therapy? Nat Rev Cancer 2:826–835. doi:10.1038/nrc925
33. Carmeliet P, Jain RK (2000) Angiogenesis in cancer and other diseases. Nature 407:249–257. doi:10.1038/35025220
34. Jain RK (2005) Normalization of tumor vasculature: an emerging concept in antiangiogenic therapy. Science 307:58–62. doi:10.1126/science.1104819